PAPER • OPEN ACCESS

Design and validation of a sliding mode disturbance observer-based control for a CubesSat nano-satellite

To cite this article: Amr M. Hassan and Ayman A. ElBadawy 2019 *IOP Conf. Ser.: Mater. Sci. Eng.* **610** 012035

View the article online for updates and enhancements.

Design and validation of a sliding mode disturbance observer-based control for a CubesSat nano-satellite

Amr M.Hassan[1] and Ayman A. ElBadawy[1, 2*]

[1] Mechatronics Engineering Department, German University in Cairo, Cairo, Egypt
[2] Mechanical Engineering Department, Al-Azhar University, Cairo, Egypt

[*]ayman.elbadawy@guc.edu.eg

Abstract. Cubesat-class nanosatellites are characterized by their inexpensive cost of manufacturing and launch; thus, have gained a lot of interest in research recently. An actuator model for the three Magnetorquers and three reaction wheels is derived, as well as the kinematical and dynamical model of the Cubesat, for implementing an Attitude Determination and Control System (ADCS). Two different control approaches are investigated. Firstly, a Quaternion Feedback (QF) algorithm is derived and applied to assess the response of the system. Furthermore, a Sliding Mode Disturbance Observer-Based Control (SMDO) is implemented to achieve robustness against the un-modeled dynamics represented in the high coupling between the reaction wheels and the satellite dynamics. The SMDO controller has reduced the oscillations in the states response as well as the stabilization time in comparison to the QF controller. Finally, the effectiveness of SMDO has shown a significant decrease in the control effort compared to conventional sliding mode control.

1. Introduction

The launch of the first satellite Sputnik in October 1957, was the start of space exploration and space discovery missions. The field of space research have been of interest to many scientists and engineers all around the globe. However, space exploration is very expensive and requires a massive amount of money and resources as the cost of putting on pound of materials in the low earth orbits (LEO) is about 10,000 USD and it costs 500 to 700 million USD on each shuttle mission [1]. The budget for NASA missions and research have been growing each year to reach 19,2805 Million USD in 2016 [2]. Due to the high cost of designing and manufacturing of a full-size satellite which ranges between 50 and 500 Millions USD, the research in satellite designs and testing have been very low and have been avoided, and so the need for a new class of satellites with a manufacturing and launch cost of reasonable values for academic institutions. Hence, the development of the small satellite class was established.

Small satellite class can be broken down to 5 sub-classes, which are categorized according to their weight; Minisatellite (100 - 180 kg), Microsatellite (10 - 100 kg), Nanosatellite (1 - 10 kg), Picosatellite (0.01-1kg) and finally Femtosatellite (0.001–0.01kg) [3].

The research in nanosatellites with mass 1-10 kg is currently the main focus in the section of space science and engineering research. The concept of Cubesat-class nanosatellites was firstly established in 1999 by a joint collaborative research program between Stanford University and California Polytechnic University at Space Systems Development Laboratory (SSDL) with the aim to

successfully design and construct small satellites to orbit in the low earth orbits using inexpensive and commercially available components [4].

The general standards of Cubesat-class nanosatellites are the weight range of 1-10 kg and size of $10 \times 10 \times 10 \ cm^3$ for 1U Cubesat and upwards by 10 cm increments of length [4]. The small size and weight of the Cubesat makes it possible to launch up to 3 1U Cubesats or 1 3U Cubesat at a time, from a standard deployment machine known as P-POD (Poly Picosatellite Orbital Deployer) [1].

There is an extensive literature covering different attitude control using different combinations of the commonly used actuators; Magnetorquer and Reaction wheel. In 1996, Sniewski established a sliding mode controller for a satellite actuated by a set of magnetic coils using only electromagnetic actuation [5]. In 2002, Graversen et al implemented a control design based on a constant gain approximation of a periodic system. Another control method was based on the linear matrix inequality representation of the H_2 optimal control synthesis was carried out. A considered optimal choice of actuator for the Cubesat was three magnetorquers and a momentum wheel. However, the wheel was discarded due to the space complexity, ending up with a final design of three magnetorquers [6]. In 2004, Øverby investigated three controllers --- the angular velocity feedback controller (the Wisniewski controller), the attitude controller and the linear quadratic controllers [3]. In 2005, Guerrant conducted a comparative study between two different control approaches --- B-dot and three-axis controllers [7]. In 2009, Greene from the univeristy of Toronto developed attitude determination and control subsystem (ADCS) of the GNB. Specific work on magnetorquer coil assembly, integration, and testing (AIT) and reaction wheel testing is included [8]. In 2010, Francois-Lavet implemented a combination of three magnetorquers and three reaction wheels, knowing that the accuracy of less than five degrees has never been achieved with only magnetic actuators in a nanosatellite applying a control law based on a Proportional-Derivative controller [9]. In 2011, Kjellberg at the satellite Design Laboratory at the University of Texas created a guidance, navigation, and control (GN\&C) module for a Cubesat using three magnetorquers and three reaction wheels [10]. In 2012, Kök implemented a linear controller (Linear Quadratic Regulator (LQR) and two non-linear controllers --- sliding mode control and back stepping on three different reaction wheels configurations [11]. In 2013, Li et al implemented an adaptive fuzzy sliding mode magnetic control on the Cubesat [4]. In 2016, Rondão implemented a three-axis sliding mode controller using four Reaction Wheels (pyramid configuration) and six orthogonally-oriented magnetic torque rods, two per axis [12]. In 2018, Khuller et al used a Pulsed plasma thruster (PPTs) which typically utilize a solid propellant such as polytetrafluoreothylene (PTFE) to generate moderate specific impulse at low-power scale [13]. In this paper, a sliding mode disturbance observer-based control is carried out estimating the different disturbance torques affecting the Cubesat in order to minimize the control effort.

2. Modeling
In this section the kinematical and dynamical model of the Cubesat is discussed.

2.1. Kinematical Model
The kinematics of the Cubesat will be represented as quaternion differential equations as quaternions have no singularities like the Euler angles representation. There are 2 kinematic equations available: With reference to [14] the kinematical equation can be derived and related to the angular velocity of the body:

$$\dot{q} = \begin{bmatrix} -\varepsilon^T \\ S(q) + I_{3 \times 3}\eta \end{bmatrix} \omega = \frac{1}{2}T(q)\omega \qquad (1)$$

where q is the position represented in quaternion form, $\dot{q}$ is the rate of change of the quaternion position, η is the scalar part of quaternion q_0. ε is the vector part of the quaternion $[q_1 \quad q_2 \quad q_3]$, $T(q)$ is a 4×3 skew matrix constructed from the quaternion elements expressed in equation 2 and $\omega = [\omega_x \quad \omega_y \quad \omega_z]$ is the angular velocity of the body expressed in the body frame.

$$T(q) = \begin{bmatrix} -q_1 & -q_2 & -q_3 \\ q_0 & -q_3 & -q_2 \\ q_3 & q_0 & -q_1 \\ -q_2 & q_1 & q_0 \end{bmatrix} \tag{2}$$

Equation (1) can fatherly be expressed after the separation of the vector and scalar parts of the quaternion as follows:

$$\dot{\varepsilon} = \frac{1}{2}\eta\omega - \frac{1}{2}\omega \times \varepsilon \tag{3}$$

and the scalar part can be represented in terms of the three vector components as follows:

$$\eta = q_0 = \sqrt{1 - q_1{}^2 - q_2{}^2 - q_3{}^2} = \sqrt{1 - \varepsilon_1{}^2 - \varepsilon_2{}^2 - \varepsilon_3{}^2} \tag{4}$$

and the rate of change of the quaternion scalar part is expressed as follows:

$$\dot{\eta} = -\frac{1}{2}\varepsilon^T \omega \tag{5}$$

2.2. Dynamical Model
Cubesat satellite can be treated as a rigid body rotating in space. The Dynamics of a rotating body can be described with Euler's rotation equation as follows:

$$\dot{h}_{total} = \tau_{external} - \omega \times h_{total} \tag{6}$$

where h_{total} is the total angular momentum of the body, $\tau_{external}$ is the total external torques acting on the body, which can be divided to; Magnetorquer torque τ_m, the disturbance torques $\tau_d = \tau_{gg} + \tau_{aero} + \tau_{solar}$, which are the gravity gradient, aerodynamics drag and solar radiation disturbances respectively. And the ω is the angular velocity of the body expressed in the body frame of reference. The last term is the decoupling term due to the transformation from the inertial frame to the body frame.

All satellites orbiting in LEO are subjected to inverse squared gravitational force field. This is due to the variation of the gravitational field of the earth on the satellite. The equations of the gravity gradient are derived in [14] and assuming a homogeneous distribution of the earth we get the equation[4]:

$$\tau_{gg} = \frac{3\mu}{R_0{}^3}\mu_e \times (I\mu_e) \tag{7}$$

where μ is the gravitational coefficient of the earth which value is $\mu = 3.986 \times 10^{14} \; m^3/_{s^2}$. R_0 is the distance from the center of the earth, I is the inertia matrix and μ_e is a unit vector towards the nadir.

And also are subjected to Solar Radiation torque disturbance around the centre of mass of the satellite. The equation of the Solar Radiation torque assuming complete absorption of the radiation can be expressed as [14]:

$$\tau_{solar} = \frac{F_s}{c}(1 + r)A.L \tag{8}$$

where F_s is the solar constant, c is is the speed of light, r is the solar reflectance factor, L is the center between the center of pressure and center of gravity of the satellite. The illuminated surface area is denoted by A.

Finally, they are subject to aerodynamic drag due to the collision between the air particles and the body of the satellite. This disturbance is at its maximum in low altitudes, but it is still of a significant value in the higher altitude. The aerodynamic torque acting on the satellite centre of mass is function in the area facing the air molecules. The aerodynamic drag disturbance torque equation can be expressed according to [4]:

$$\tau_{aero} = \frac{1}{2}\rho V^2 C_d A_{inc} \tag{9}$$

where ρ is the Atmospheric density (kg/m^3), A_{inc} is the perpendicular area to μ_v. Where μ_v is a unit vector in the velocity direction. C_d is the Drag coefficient, V is the velocity (m^2).

Expressing equation (6) and setting the moment of inertia of the body to be constant. The dynamical equation can be expressed as follows:

$$\frac{d}{dt}I\omega = \tau_{external} - \omega \times I\omega \tag{10}$$

$$I\dot{\omega} = \tau_c + \tau_d - S(\omega)I\omega \tag{11}$$

where $\dot{\omega}$ is the rate of change of the angular velocity of the body. τ_d is the sum of the three disturbance torques and τ_c is the control torque which is the sum of the torque provided by the two actuators; Reaction wheels and Magnetourqers.
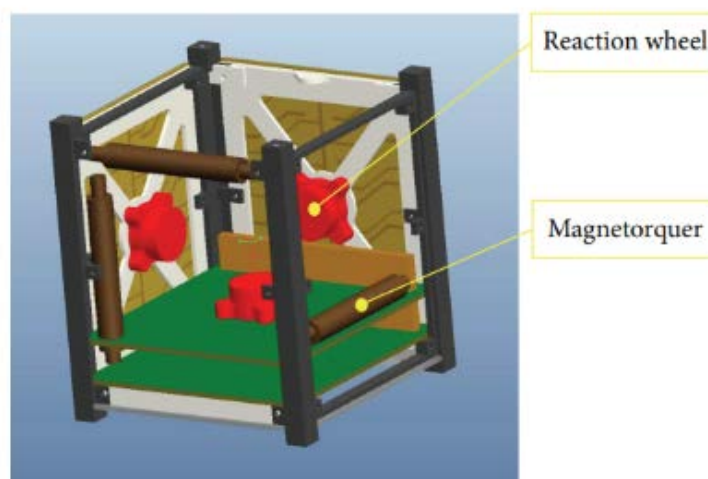
3. Methodology

Figure 1. Three Magnetorquers and three reaction wheels mounted in a Cubesat.

3.1. Magnetorquer

Magnetorquers or torque rods are coil of wire tightly around a perm-alloy material shown in Figure 1. When a current is supplied to the coil a magnetic dipole moment is induced proportional to the current, when the induced magnetic dipole moment of the Magnetorquer reacts with the magnetic field of the earth a torque is produced. The equations of the magnetic torque are based on [4] [15]. The magnetic torque is the cross product between the magnetic dipole moment and the magnetic field of the Earth as follows:

$$\vec{\tau} = \vec{M} \times \vec{B} \tag{12}$$

$\vec{\tau}$ is the torque vector induced, $\vec{M}$ is the magnetic dipole moment of the coils and $\vec{B} = [B_x \quad B_y \quad B_z]$ is the vector of the magnetic field of the Earth. The magnetic dipole moment is expressed as follows:

$$M_k = N_k i_k A_k \tag{13}$$

M is the magnetic dipole moment of the coil, N is the number of turn, i is the supplied current, A is the span area of the coil and k is the on which the coil is mounted; $k = x, y \text{ and } z$.

Magnetorquers are commercially available with parameters illustrated in table 1.

Table 1: Commercially available Magnetorquer parameters.

Property	Value
Life time	10 years
Dimensions	$94\ mm \times 15\ mm \times 13\ mm$
Mounting	4x M2 Socket Head Cap Screws
Mass	< 50 gm
Operating range	-10 ℃ to +50 ℃

3.2. Reaction Wheel

Reaction wheels are fly wheels mounted on the shaft of an electric motor which when the motor rotates, the satellite rotates in the opposite direction according to the principle of conservation of energy. The equations of Reaction Wheels model are based on [8] as follows:

$$\tau_{RW} = (dh_{RW}/dt) + \omega \times h_{RW} - \tau_{RW\ friction} \tag{14}$$

where τ_{RW} is the is the torque produced by the reaction wheel expressed in the body frame of reference, $h_{RW} = \begin{bmatrix} h_{RW_x} & h_{RW_y} & h_{RW_z} \end{bmatrix}^T = I_{RW}\omega_{RW}$ is the angular momentum of the reaction wheels, ω is the angular velocity of the satellite expressed in the body frame and $\tau_{RW\ friction}$ is the friction torque of the reaction wheel. For simplicity and due to its negligible value, $\tau_{RW\ friction}$ is ignored in our simulation. With accordance to the energy conservation principle, a torque rotating the reaction wheels will produce a torque rotating the satellite with the same magnitude but in different direction as illustrated in equation (15).

$$I_{RW}\omega_{RW} = -I\omega \tag{15}$$

The equation of the Reaction wheel can be expressed as follows:

$$\tau_{RW} = (dh_{RW}/dt) + \omega \times h_{RW} = \begin{bmatrix} \dot{h}_{RWx} + h_{RWz}\omega_y - h_{RWy}\omega_z \\ \dot{h}_{RWy} + h_{RWx}\omega_z - h_{RWz}\omega_x \\ \dot{h}_{RWz} + h_{RWy}\omega_x - h_{RWx}\omega_y \end{bmatrix} \qquad (16)$$

by adding the Reaction wheel elements in the dynamics (11) the equation is expressed as follows:

$$\dot{\omega} = I^{-1}(\tau_c + \tau_d - S(\omega)I\omega - S(\omega)h_\omega) \qquad (17)$$

4. Control Approach

Two control approaches investigated on the model; Quaternion feedback and Sliding mode disturbance observer based control (SMDO).

4.1. Quaternion Feedback

The attitude control using the Quaternion Feedback approach requires the calculation of the deviation of the attitude of the satellite from a desired attitude, this calculation is the quaternion error calculation. Since the orientation of the body is described in three dimensions, simply subtracting the actual attitude from the desired to get the error will not result in a valid error.

Supposing to have a rotation matrix R_d which describes the desired attitude of the satellite and a rotation matrix R which is the actual orientation of the body, the deviation (error) between the desired and the actual is described by the rotation matrix $\tilde{R}$. Where $\tilde{R} \epsilon SO(3)$ defined by $\tilde{R} = R_d^T$, $R(\tilde{q}) = R^T(q_d^*)R(q) = R(q_d^*)R(q)$ where q_d is the desired quaternion and q_d^* is the complex conjugate of q_d. q is the actual quaternion of the body and $\tilde{q}$ is the error deviation of the body. Therefore, $R(\tilde{q}) = R(q_d^*)R(q) = R(q_d^* \otimes q)$, where $\otimes$ is the quaternion product operator. The quaternion error can be expressed as follows:

$$\tilde{q} = q_d^* \otimes q = \begin{bmatrix} \eta_d & \varepsilon_d^T \\ -\varepsilon_d & \eta_d I_{3\times 3} - S(\varepsilon_q)q \end{bmatrix} = \begin{bmatrix} \eta_d \eta + \varepsilon_d^T \varepsilon \\ \eta_d \varepsilon - \eta \varepsilon_d - \varepsilon_d \times \varepsilon \end{bmatrix} \qquad (18)$$

The attitude error quaternion vector consists of the last three elements of $\tilde{q}$:

$$\tilde{\varepsilon} = \eta_d \varepsilon - \eta \varepsilon_d - \varepsilon_d \times \varepsilon \qquad (19)$$

The derivative of the error is expressed as follows:

$$\dot{\tilde{\varepsilon}} = \dot{\eta}_d \varepsilon + \eta_d \dot{\varepsilon} - \dot{\eta}\varepsilon_d - \eta\dot{\varepsilon}_d - \dot{\varepsilon}_d \times \varepsilon - \varepsilon_d \times \dot{\varepsilon} \qquad (20)$$

and the non-linear PD control law equation using equations 19 and 20 is expressed as follows:

$$\tau_{control} = -K_p \tilde{\varepsilon} - K_d \dot{\tilde{\varepsilon}} \qquad (21)$$

where $\tau_{control}$ is the control torque from the controller, K_p is the positive proportional gain and K_d is the positive derivative gain.

4.2. Sliding Mode Disturbance Observer Based Control (SMDO)

A Sliding Mode Disturbance Observer Based Control (SMDO) is implemented to achieve robustness against the un-modeled dynamics represented in the high coupling between the actuator (Reaction Wheel) and the satellite dynamics.

4.2.1. Sliding Manifold. The design of the SMC is divided into two parts --- the sliding manifold and the control law.Firstly the manifold is designed and in the next section the control law is defined.

The sliding manifold used is expressed in equation 22 [11].

$$s = \omega + \lambda q_e \tag{22}$$

Lyapunov candidate function is expressed as:

$$V = \frac{1}{2}s^T s \tag{23}$$

The Lyapunov function derivative is expressed as follows:

$$\dot{V} = \frac{1}{2}\dot{s}^T s + \frac{1}{2}s^T \dot{s} = s^T \dot{s} \tag{24}$$

$$\dot{V} = s^T(\dot{\omega} + \lambda \dot{q_e}) \tag{25}$$

substituting equation (17) in (25) results in:

$$\dot{V} = s^T I^{-1}(-S(\omega)(I\omega + h_\omega) + \tau_c + \tau_d + I\lambda \dot{q_e}) \tag{26}$$

4.2.2. Control Law. The control law is chosen as $\tau = \mu_{eq} - Ksign(s)$ where an adequate u_{eq} is designed to cancel out all the dynamics in 17. After the substitution, the derivative of V being negative definite guarantees the asymptotically stability of the sliding surface. Therefore μ_{eq} will be expressed as follows :

$$\mu_{eq} = I\dot{\omega} + S(\omega)I\omega + S(\omega)h_\omega - \tau_d \tag{27}$$

therefore the control torque of the SMDO can be expressed as follows:

$$\tau_c = I\dot{\omega} + S(\omega)I\omega + S(\omega)h_\omega - \tau_d - Ksign(s) \tag{28}$$

4.3. Disturbance Observer

Considering a class of nonlinear systems, depicted by

$$\dot{x} = f(x) + g_1(x)u + g_2(x)d \tag{29}$$

where $x \in R^n$, $u \in R^m$, $d \in R^l$ are the states, the control input and the disturbance respectively. To estimate the unknown disturbances d, a nonlinear disturbance observer is suggested as:

$$\dot{\hat{d}} = l(x)[\dot{x} - f(x) - g_1(x)u - g_2(x)\hat{d}] \tag{30}$$

where $\hat{d}$ denotes the disturbance estimation vector, and $l(x)$ is the nonlinear gain function of observer. The disturbance estimation error is defined as:

$$e_d = \hat{d} - d \tag{31}$$

combining equation 29, 30 and 31 the dynamics of disturbance estimation error are obtained, which are governed by

$$\dot{e}_d = \dot{\hat{d}} - \dot{d} \tag{32}$$

$$\dot{e}_d = l(x)[\dot{x} - f(x) - g_1(x)u - g_2(x)\hat{d}] \tag{33}$$

$$\dot{e}_d = -l(x)g_2(x)e_d + \dot{d} \tag{34}$$

which implies that the disturbance estimation error will converge to zero as time goes to infinity if the observer gain $l(x)$ is chosen such that system is asymptotically stable. $l(x)$ is chosen to be a $\mathbf{3 \times 6}$ illustrated in equation 35 matrix with three gains multiplied in the three angular velocities $\boldsymbol{\omega_x, \omega_y}$ $\boldsymbol{and}$ $\boldsymbol{\omega_z}$ as the angular velocities are related to the quaternion angles shown in equation 1. The $\dot{\boldsymbol{d}}$ term is excluded from the equation in case of constant disturbances estimation.

$$l(x) = \begin{bmatrix} 0 & 0 & 0 \\ 0 & 0 & 0 \\ 0 & 0 & 0 \\ \lambda_1 & 0 & 0 \\ 0 & \lambda_2 & 0 \\ 0 & 0 & \lambda_3 \end{bmatrix} \tag{35}$$

studying the stability of the nonlinear observer after choosing $l(x)$ is done using Lyaponov:

$$v = \frac{1}{2}e_d^T e_d \tag{36}$$

$$
\begin{aligned}
\dot{v} &= \frac{1}{2}e_d^T \dot{e}_d \\
&= -e_d^T l(x)g_2(x)e_d \\
&= -\begin{bmatrix} e_{dx} & e_{dy} & e_{dz} \end{bmatrix} \begin{bmatrix} 0 & 0 & 0 \\ 0 & 0 & 0 \\ 0 & 0 & 0 \\ \lambda_1 & 0 & 0 \\ 0 & \lambda_2 & 0 \\ 0 & 0 & \lambda_3 \end{bmatrix} \begin{bmatrix} 0 & 0 & 0 \\ 0 & 0 & 0 \\ 0 & 0 & 0 \\ 1/I_x & 0 & 0 \\ 0 & 1/I_y & 0 \\ 0 & 0 & 1/I_z \end{bmatrix} \begin{bmatrix} e_{dx} \\ e_{dy} \\ e_{dz} \end{bmatrix} \\
&= -\lambda_1 \frac{1}{I_x}e_{dx}^2 - \lambda_2 \frac{1}{I_y}e_{dy}^2 - \lambda_3 \frac{1}{I_z}e_{dz}^2
\end{aligned}
\tag{37}
$$

so that if the observer gains $\boldsymbol{\lambda_1, \lambda_2}$ $\boldsymbol{and}$ $\boldsymbol{\lambda_3}$ are chosen to be negative, the rate of change of the Lyapunov function will be negative definite which guarantee the asymptotic stability of the nonlinear observer.

5. Results

The mathematical model presented in this paper is simulated using MATLAB/SIMULINK In simulations, it is assumed that the attitude of the satellites continuously provided by determination system without errors. The satellite simulation parameters are illustrated in table 2.

Table 2: MATLAB simulation parameters.

Parameters	Value
Satellite Inertia Matrix (I)	$diag(0.01, 0.01, 0.01)kgm^2$
Orbit	600km
Reaction Wheel Inertia	43×10^{-5} (one wheel)
Max. Reaction wheel torque	75×10^{-4}
Max. Magnetorquer dipole	$0.2Am^2$
Simulation time & 500 seconds	500 seconds
$\omega_{initial}$	$[0 \quad 0 \quad 0]^T$

5.1. Quaternion Feedback

A QF algorithm is conducted to assess the response of the system. Starting from a specific initial quaternion corresponding to Euler angles $[59.04 \quad 38.17 \quad 30.96]^T$ with a proportional gain parameter $k_p = 15$ and Derivative Gain Parameter $k_d = 250$ reaching a desired Euler angles of $[\phi \quad \theta \quad \varphi] = [0 \quad 0 \quad 0]^T$.
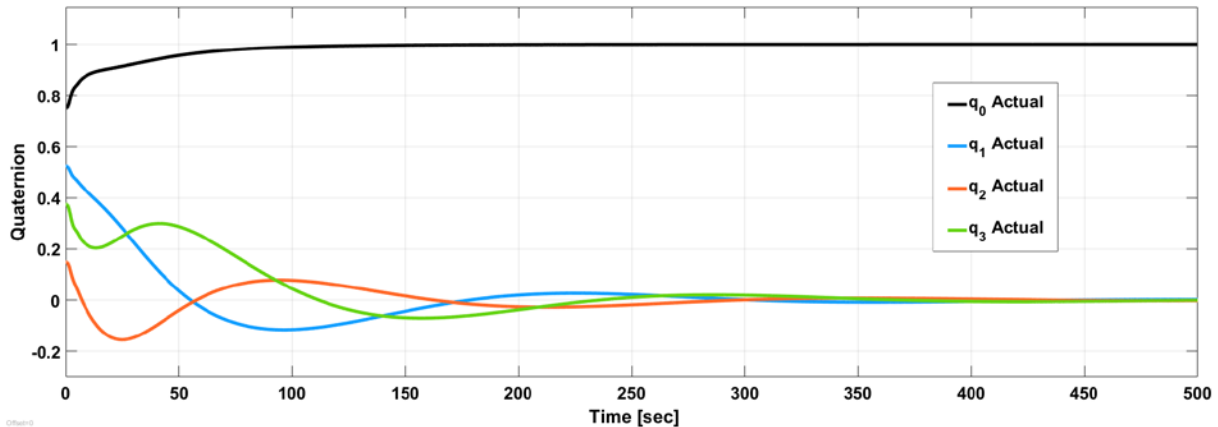

Figure 2: Cubesat stabilization using QF.

The Quaternion feedback succeeded in stabilizing the Cubesat pointing to a specific point in space shown in figure 2 represented by specific Roll, Pitch and Yaw to be $[0 \quad 0 \quad 0]^T$ starting from initial Euler angles $[59.04 \quad 38.17 \quad 30.96]^T$ against the disturbance torques with a Root Mean Square Error of 0.0144 and rise time of 180 seconds.

5.2. Sliding Mode Disturbance Observer Based Control (SMDO)

As discussed before there are three main disturbances acting on the Cubesat two constant disturbances: τ_{gg} and τ_{solar} and one harmonic disturbance τ_{aero}. A nonlinear Disturbance Observer is implemented to estimate both disturbances to deal with uncertain parameters of the actual disturbance and in order to decrease the control effort of the controller. Gravity Gradient Torque τ_{gg} and Solar Radiation Torque τ_{solar} are considered as constant disturbances as they are their variation at the same altitude could be negligible shown in figure 3.
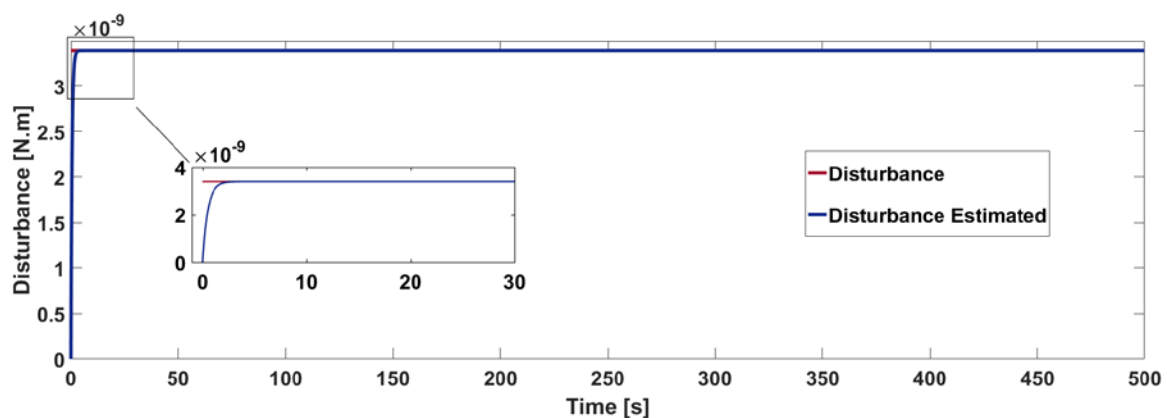

Figure 3: Gravity Gradient Torque τ_{gg} and Solar Radiation Torque τ_{solar} estimated disturbance Vs the actual disturbance.

The Disturbance Observer succeeded in estimating both constant disturbances with a Root Mean Square Error (RMSE) of 3×10^{-11} and rise time of 1.073 seconds.

For an elliptical orbit aerodynamic drag torque τ_{aero} is periodic and its variation cannot be neglected as shown in figure 4.
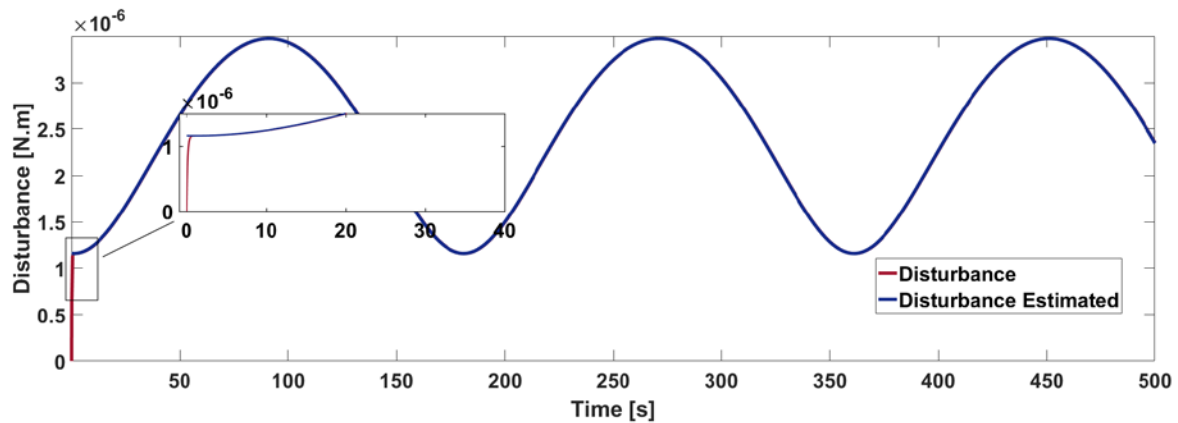

Figure 4: Aerodynamic drag torque τ_{aero} estimated disturbance Vs the actual disturbance.

The Disturbance Observer also succeeded in estimating the periodic disturbance with a Root Mean Square Error (RMSE) of 1.3×10^{-8} and rise time of 1.3 seconds.

Implementing SMDO starting from a specific initial quaternion corresponding to Euler angles $[59.04 \quad 38.17 \quad 30.96]^{T}$ reaching a desired Euler angles of $[\phi \quad \theta \quad \varphi] = [0 \quad 0 \quad 0]^{T}$.
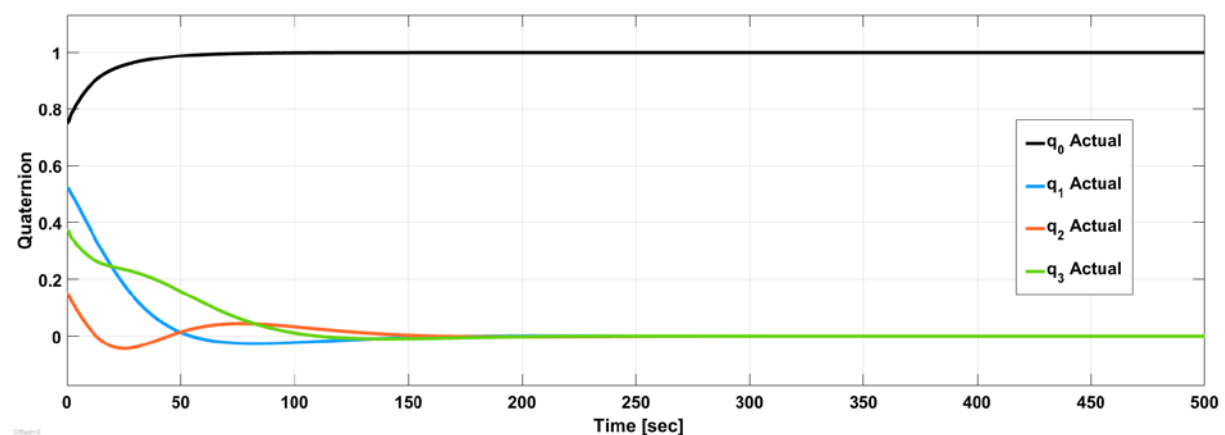

Figure 5: Cubesat stabilization using SMDO.

The Sliding mode disturbance observer based control succeeded in stabilizing the Cubesat pointing to a specific point in space shown in figure 5 represented by specific Roll, Pitch and Yaw to be

$[\,0 \quad 0 \quad 0\,]^{T}$ starting from initial quaternion corresponding to Euler angles $[59.04 \quad 38.17 \quad 30.96]^{\mathrm{T}}$ against the disturbance torques with a Root Mean Square Error of 0.001 and rise time of 53 seconds which is better than that of the quaternion feedback.

A validation of decreasing the control effort after the disturbance observer implementation was conducted by calculating the control effort with and without the DOB implementation and calculate the percentage difference between them relative to the disturbance applied to the system.
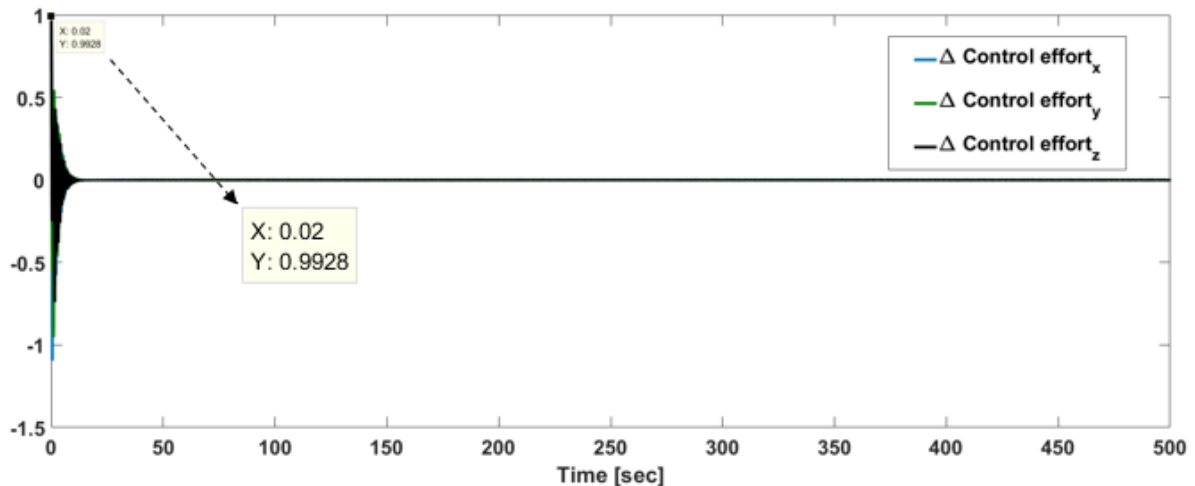

Figure 6: Difference in control effort with and without DOB implementation.

It is found in figure 6 that the percentage of difference of the control effort with and without DOB implementation relative to the disturbance is unity that refers to increasing the control effort by the value of disturbance in case of not implementing DOB. This validates the disturbance observer advantage in decreasing the control effort.

6. Conclusion
In this paper, two control approaches were implemented on the system; QF algorithsm succeeded in stabilizing the Cubesat against the disturbance torques with a Root Mean Square Error of 0.0144 and rise time of 180 seconds. Furthermore, robustness is also provided against un-modeled dynamics by implementing SMDO that succeeded in stabilizing the system with a Root Mean Square Error of 0.001 and rise time of 53 second. This approach added chattering effect to the system that can be reduced by smoothing the discontinuous function in the cost of the robustness. The effectiveness of estimating the disturbance is validated to reduce the control effort relative to the conventional sliding mode control.

7. References

[1]   M. Kaku, "The Cost Of Space Exploration," *Forbes*. 2009.
[2]   J. Wilson, "Budget Documents, Strategic Plans and Performance Reports." 2013.
[3]   E. J. Øverby, "Attitude control for the Norwegian student satellite nCube," *Eng. Cybern.*, p. 108, 2004.
[4]   J. Li, "Design of Attitude Control Systems for CubeSat-Class Nanosatellite," *J. Control Sci. Eng.*, vol. 27, no. 3, pp. 571–582, 2013.
[5]   D. Thesis, "Satellite Attitude Control Using Only Electromagnetic Actuation Rafał Wi´ sniewski.pdf."

[6]   T. Graversen, M. K. Frederiksen, and S. V. Vedstesen, "Attitude Control system for AAU CubeSat," *Current*, no. june, p. 112, 2002.

[7]   D. V. Guerrant, "Design and Analysis of Fully Magnetic Control for Picosatellite Stabilization," *Calif. Polytech. State Univ.*, no. June, p. 143, 2005.

[8]   M. R. Greene, "The Attitude Determination and Control System of the Generic Nanosatellite Bus," 2009.

[9]   V. Francois-Lavet, "Study of passive and active attitude control systems for the OUFTI nanosatellites," *Math. Model.*, 2010.

[10]   H. C. Kjellberg, "Design of a CubeSat Guidance , Navigation , and Control Module by Henri Christian Kjellberg," no. August 2011, 2015.

[11]   I. Kök, "Comparison and Analysis of Attitude Control Systems of a Satellite Using Reaction Wheel Actuators," pp. 17–18, 2012.

[12]   D. O. de M. A. Rondao, "Modeling and Simulation of the ECOSat-III Attitude Determination and Control System," no. April, 2016.

[13]   A. R. Khuller *et al.*, "Pulsed Plasma Thruster for Multi-Axis CubeSat Attitude Control Applications," no. July, pp. 0–33, 2018.

[14]   S. KARATAŞ, "LEO SATELLITES: DYNAMIC MODELLING, SIMULATIONS AND SOME NONLINEAR ATTITUDE CONTROL TECHNIQUES," 2006.

[15]   C. Kaplan, "Leo Satellites Attitude Determination and Control Components," no. April, p. 192, 2006.